Sensitivity to thermal noise of atomic Einstein-Podolsky-Rosen entanglement

R. J. Lewis-Swan and K. V. Kheruntsyan

School of Mathematics and Physics, The University of Queensland, Brisbane, Queensland 4072, Australia

We examine the prospect of demonstrating Einstein-Podolsky-Rosen (EPR) entanglement for massive particles using spin-changing collisions in a spinor Bose-Einstein condensate. Such a demonstration has recently been attempted by Gross *et al.* [Nature (London) **480**, 219 (2011)] using a condensate of ^{87}Rb atoms trapped in an optical lattice potential. For the condensate initially prepared in the $(F, m_F) = (2,0)$ hyperfine state, with no population in the $m_F = \pm 1$ states, we predict a significant suppression of the product of inferred quadrature variances below the Heisenberg uncertainty limit, implying strong EPR entanglement. However, such EPR entanglement is lost when the collisions are initiated in the presence of a small (currently undetectable) thermal population $\bar{n}_{\text{th}}$ in the $m_F = \pm 1$ states. For condensates containing 150–200 atoms, we predict an upper bound of $\bar{n}_{\text{th}} \simeq 1$ that can be tolerated in this experiment before EPR entanglement is lost.

I. INTRODUCTION

Entanglement has proven to be "the characteristic trait of quantum mechanics" as first coined by Schrödinger [1]. It forms the foundations of quantum information theory and quantum computing. Further, in interferometry entanglement enables measurement precision to surpass the standard quantum limit [2]. This is particularly important in atom interferometry [3] as atom flux is generally limited. However, the most important foundational trait of entanglement comes with its role in the Einstein-Podolsky-Rosen (EPR) paradox [4]. This requires the underlying quantum correlations to be stronger than those satisfying the simpler inseparability criteria. The resulting EPR-entanglement criterion confronts the Heisenberg uncertainty relation and puts us into the context of EPR arguments that question the completeness of quantum mechanics and open the door to alternative descriptions of these correlations via local hidden-variable theories [5]. The EPR paradox for continuous-variable quadrature observables [6] (which are analogous to the position and momentum observables originally discussed by Einstein, Podolsky, and Rosen) has been demonstrated in optical parametric down-conversion [7] and most recently attempts have been made to demonstrate [8] the paradox with ensembles of massive particles generated by spin-changing collisions in a spinor Bose-Einstein condensate (BEC) [9,10].

In this paper we seek to provide a theoretical treatment of the recent experiment by Gross *et al.* [8], which reported entanglement, or quantum inseparability, of two atomic ensembles produced by spin-changing collisions in a ^{87}Rb BEC. For the BEC initially prepared in the $(F, m_F) = (2,0)$ hyperfine state, the collisions produce correlated pairs of atoms in the $m_F = \pm 1$ sublevels. The authors observed that the resulting state was inseparable, though a measurement of a stronger EPR-entanglement criterion was inconclusive. A normalized product of inferred quadrature variances of 4 ± 17 was reported, whereas a demonstration of the EPR paradox requires this quantity to be less than unity [6,11].

The short-time dynamics of the spin-mixing process, for a vacuum initial state of the $m_F = \pm 1$ atoms, is similar to that of a spontaneous parametric down-conversion in the undepleted pump approximation. This paradigmatic nonlinear

optical process is known to produce an EPR-entangled twin-photon state that can seemingly violate the Heisenberg uncertainty relation for inferred optical quadratures [6]. Such a violation was previously observed by Ou *et al.* [7]. Due to the inconclusive nature of an analogous measurement of matter-wave quadratures in Ref. [8], we seek to perform a theoretical analysis of spin-changing dynamics and calculate various measures of entanglement in experimentally realistic regimes. In particular, we focus on the sensitivity of EPR entanglement to an initial population in the $m_F = \pm 1$ sublevels with thermal statistics. In the optical case this question is argued to be irrelevant as at optical frequencies and room temperatures the thermal population of the signal and idler modes is negligible, allowing us to safely approximate them as vacuum states. However, these considerations are inapplicable to ultracold atomic gases. This was highlighted recently by Melé-Messeguer *et al.* [12], who quantitatively predicted the possibility of nontrivial thermal activation of the $m_F = \pm 1$ sublevels in a spin-1 BEC. Accordingly, when interpreting experimental results care must be taken in differentiating spin-mixing dynamics initiated by vacuum noise from that initiated by thermal noise or a small coherent seed [13]. To this end, our modeling of the experiment of Gross *et al.* [8] is more consistent with a small thermal population in the $m_F = \pm 1$ sublevels rather than a vacuum initial state or small coherent seed. From a broader perspective, the connection between our results and the widely applicable model of parametric down-conversion highlights the generally fragile nature of atomic EPR entanglement to thermal noise, demonstrating that future experiments must be refined to overcome this problem.

II. SYSTEM

The experiment of Ref. [8] starts with a BEC of ^{87}Rb atoms prepared in the $(F, m_F) = (2,0)$ state and trapped in a one-dimensional optical lattice. The lattice potential is sufficiently deep to prevent tunneling between neighboring wells. Furthermore, due to the relatively small number of atoms in each well, the spin-healing length is of the order of the spatial size of the condensate in the well, meaning the spatial dynamics of the system are frozen, and hence

we may treat the condensate in each well according to the single-mode approximation [14–16]. In this approximation the field operator $\hat{\psi}_i(\mathbf{r})$ for each component $i \equiv m_F = 0, \pm 1, \pm 2$ is expanded as $\hat{\psi}_i(\mathbf{r}) = \phi(\mathbf{r})\hat{a}_i$, where $\phi(\mathbf{r})$ is the common spatial ground-state wave function [$\phi_i(\mathbf{r}) \equiv \phi(\mathbf{r})$] and $\hat{a}_i$ is the respective bosonic annihilation operator.

A quadratic Zeeman shift and microwave dressing of the $m_F = 0$ state is employed to energetically restrict the spin-mixing dynamics to the $m_F = 0, \pm 1$ states [8] and so for short-time durations we may map the spin-2 system to an effective spin-1 Hamiltonian [17] of the form $\hat{H} = \hat{H}_{\text{inel}} + \hat{H}_{\text{el}} + \hat{H}_Z$,

$$\hat{H}_{\text{inel}} = \hbar g(\hat{a}_0^\dagger \hat{a}_0^\dagger \hat{a}_{-1} \hat{a}_1 + \hat{a}_1^\dagger \hat{a}_{-1}^\dagger \hat{a}_0 \hat{a}_0), \tag{1}$$

$$\hat{H}_{\text{el}} = \hbar g(\hat{n}_0 \hat{n}_1 + \hat{n}_0 \hat{n}_{-1}), \tag{2}$$

$$\hat{H}_Z = -p(\hat{n}_1 - \hat{n}_{-1}) - q(\hat{n}_1 + \hat{n}_{-1}), \tag{3}$$

where $\hat{n}_i = \hat{a}_i^\dagger \hat{a}_i$ is the particle number operator and $i = 0, \pm 1$ are herein referred to as the pump and the signal and idler modes, respectively. We have ignored terms proportional to $\hat{N}(\hat{N} - 1)$ in $\hat{H}$ as this is a conserved quantity and contributes only a global phase rotation. The inelastic spin-changing collisions are described by $\hat{H}_{\text{inel}}$ and the remaining elastic s-wave scattering terms are grouped in $\hat{H}_{\text{el}}$, where g is the coupling constant associated with s-wave collisions [17]. For a spin-2 system, the coupling is given by $g = \frac{6}{14}(3g_4 + 4g_2) \int d^3\mathbf{r} |\phi(\mathbf{r})|^4$, where $g_F = 4\pi\hbar^2 a_F/m$ describes s-wave scattering with total spin F, characterized by scattering length a_F [17]. For comparison, for an actual spin-1 system the coupling constant would be given by $g = \frac{g_2 - g_0}{3} \int d^3\mathbf{r} |\phi(\mathbf{r})|^4$, where $g_F = 4\pi\hbar^2 a_F/m$. In our representation of $\hat{H}_{\text{el}}$ we have used the fact that the relative number difference $\hat{n}_1 - \hat{n}_{-1}$ is a conserved quantity. The interaction with the magnetic field is described by $\hat{H}_Z$, where the linear and quadratic Zeeman effects are parametrized, respectively, by $p = \mu_B B_0/2$ and $q = p^2/\hbar\omega_{\text{HFS}}$ [18], with $\omega_{\text{HFS}}/2\pi \approx 6.835$ GHz being the hyperfine splitting frequency of ^{87}Rb [19]. For our initial conditions the relative number difference $\hat{n}_1 - \hat{n}_{-1}$ will always be zero and hence we may ignore the linear Zeeman effect. We may also redefine the parameter q to absorb the effects of microwave level dressing (used by Gross *et al.* [8]) and any other fixed energy shift between the $m_F = 0$ and ± 1 energy levels.

Simple analogies between the states of the signal and idler modes in spin-changing collisions and optical parametric down-conversion consider only $\hat{H}_{\text{inel}}$ in the undepleted pump approximation; however, competing mean-field ($\hat{H}_{\text{el}}$) and Zeeman ($\hat{H}_Z$) effects lead to additional dynamics [20] due to dephasing. The full Heisenberg operator equations of motion are given by

$$\frac{d\hat{a}_0}{d\tau} = -i[2\hat{a}_{-1}\hat{a}_1\hat{a}_0^\dagger + (\hat{n}_1 + \hat{n}_{-1})\hat{a}_0], \tag{4}$$

$$\frac{d\hat{a}_{\pm 1}}{d\tau} = -i[\hat{a}_0^2 \hat{a}_{\mp 1}^\dagger + (\hat{n}_0 - q/g)\hat{a}_{\pm 1}], \tag{5}$$

where we have introduced $\tau = gt$ as dimensionless time. We see that the phase accrued in the $\hat{a}_{\pm 1}$ modes grows proportionally to $\hat{n}_0 - q/g$, while for the $\hat{a}_0$ mode the phase grows proportionally to $\hat{n}_1 + \hat{n}_{-1}$. In the short-time undepleted pump approximation [21], this is equivalent to a phase rotation

$\hat{a}_{\pm 1} \rightarrow \hat{a}_{\pm 1}\exp[i(N_0 - q/g)\tau]$, where $N_0 = \langle \hat{n}_0(0) \rangle$ is the initial population of the $m_F = 0$ component. This rotation leads to a dynamical phase mismatch between the spinor components that decelerates the pair-production process [20]. To prevent phase mismatch in the short-time limit one can choose $q = gN_0$, in which case Eqs. (4) and (5) reduce to those of resonant down-conversion [21].

III. RESULTS AND DISCUSSION

A. Population dynamics

We first analyze the spin-changing dynamics for the case of a vacuum initial state for the signal and idler modes and a coherent state $|\alpha_0(0)\rangle$ for the pump mode with an initial number of atoms $N_0 = |\alpha_0(0)|^2$. This case can be treated in a straightforward manner (see, e.g., Ref. [11]) by diagonalizing the full Hamiltonian in the truncated Fock-state basis and solving the Schrödinger equation (see also [22]). Figure 1(a) shows the population dynamics of the signal and idler modes for different initial atom numbers N_0 and the quadratic Zeeman term tuned to the phase-matching condition $q = gN_0$. Setting $q = 0$ eliminates the Zeeman shift and we observe (gray solid line) significantly slowed dynamics due to phase mismatch. For reference, we also mark the experimental measurement time of Ref. [8], $\tau' = 0.0073$, corresponding to the reported value of the squeezing parameter $r \equiv N_0\tau' \simeq 2$ [21], evaluated for $N_0 = 275$.

We next analyze the case of an initial thermal seed in the signal and idler modes, with an equal average number of atoms $\bar{n}_{\text{th}}$ in both modes. To simulate the dynamics in this case, we use the truncated Wigner method (Ref. [23] gives simple prescriptions on how to model various initial states in the Wigner representation). Figure 1(b) illustrates that the presence of the thermal seed accelerates population growth, however, it does not significantly effect the maximal depletion of the BEC. The numerical results in Fig. 1(b)
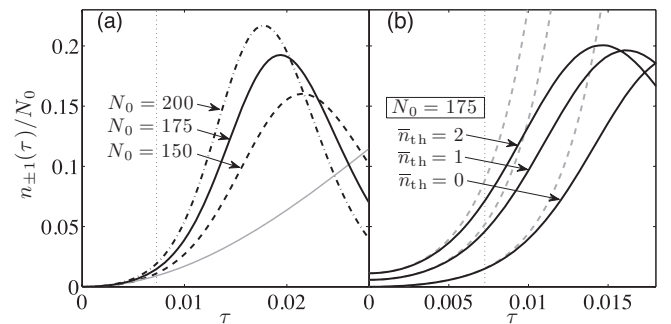

FIG. 1. (a) Fractional population $n_{\pm 1}(\tau)/N_0$ of the signal and idler modes [where $n_{\pm 1}(\tau) \equiv \langle \hat{a}_{\pm 1}^\dagger(\tau)\hat{a}_{\pm 1}(\tau) \rangle$] as a function of the dimensionless time τ for the vacuum initial state and different initial number of atoms in the pump mode N_0. The quadratic Zeeman term is phase matched to $q = gN_0$ in all cases, except for the gray solid line, which is shown for comparison for $q = 0$ and $N_0 = 175$. The vertical dotted line indicates the measurement time $\tau' = 0.0073$ used in Ref. [8]. (b) Same as in (a), but with thermally seeded populations in the signal and idler modes (assumed to be equal to each other) for $N_0 = 175$. The gray dashed lines show the analytic predictions in the undepleted pump approximation.

are compared with the analytic predictions of the simple model of parametric down-conversion in the undepleted pump approximation $n_{\pm 1}(\tau) = \sinh^2(N_0\tau)[1 + 2\bar{n}_{\text{th}}] + \bar{n}_{\text{th}}$ (see the Appendix for full analytic solutions). As expected, we find good agreement between the numerical and analytic results in the short-time limit. We also conclude that as far as the mode populations are concerned, the experimental measurement time $\tau' = 0.0073$ is not too far from the regime of validity of the simple analytic model, at least for $\bar{n}_{\text{th}} \lesssim 2$. This conclusion, however, cannot necessarily be carried through to other observables such as the entanglement measures analyzed below.

B. Einstein-Podolsky-Rosen entanglement

Central to this paper is an investigation into the possible demonstration of the EPR paradox as outlined in Ref. [8]. In the context of continuous-variable entanglement, this is equivalent to the seeming violation of the Heisenberg uncertainty relation for inferred quadrature variances [6,11]. In the normalized form this EPR-entanglement criterion can be written as

$$\Upsilon_j = \frac{\Delta^2_{\text{inf}}\hat{X}_j \Delta^2_{\text{inf}}\hat{Y}_j}{(1 - \langle \hat{a}^\dagger_j \hat{a}_j \rangle / \langle \hat{b}^\dagger_j \hat{b}_j \rangle)^2} < 1, \qquad (6)$$

where the optimal[1] inferred quadrature variance for $\hat{X}_j$ (and similarly for $\hat{Y}_j$) is given by [6]

$$\Delta^2_{\text{inf}}\hat{X}_j = \langle(\Delta\hat{X}_j)^2\rangle - \frac{\langle\Delta\hat{X}_i\Delta\hat{X}_j\rangle^2}{\langle(\Delta\hat{X}_i)^2\rangle}, \qquad (7)$$

with $\Delta\hat{X}_j \equiv \hat{X}_j - \langle\hat{X}_j\rangle$ and $i,j = \pm 1$. The generalized quadrature operators are defined as $\hat{X}_j(\theta) = (\hat{a}^\dagger_j\hat{b}_j e^{i\theta} + \hat{b}^\dagger_j\hat{a}_j e^{-i\theta})/\langle\hat{b}^\dagger_j\hat{b}_j\rangle^{1/2}$ [11], where the operator $\hat{b}_j$ represents the local oscillator field required for homodyne detection of the quadratures and we define $\hat{X}_j = \hat{X}_j(\pi/4)$ and $\hat{Y}_j = \hat{X}_j(3\pi/2)$. Choosing this pair of canonically conjugate quadratures maximizes the correlation (anticorrelation) between them, defined as $C = \langle\hat{X}_i(\theta)\hat{X}_j(\theta)\rangle/[\langle\hat{X}_i(\theta)^2\rangle\langle\hat{X}_j(\theta)^2\rangle]^{1/2}$, thus minimizing the inferred quadrature variance.

Our choice of generalized quadrature operators [11] varies from the standard form $\hat{X}_j(\theta) = \hat{a}_j e^{-i\theta} + \hat{a}^\dagger_j e^{i\theta}$ [21], as it does not assume a perfectly coherent, strong local oscillator. Instead, it takes into account the fact that the local oscillator is derived, just before the measurement time, from the partially depleted and already incoherent pump mode [8]. When measuring these quadratures the pump mode is split into two local oscillators by an atomic beam splitter [11] (for instance, a rf $\pi/2$ pulse), in which the output is given by $\hat{b}_{\pm 1} = (\hat{a}_0 \pm \hat{a}_{\text{vac}})/\sqrt{2}$, where $\hat{a}_{\text{vac}}$ represents the vacuum entering the empty port of the beam splitter. This is slightly different from

---

[1] The form of the inferred quadrature variance in Eq. (7) varies slightly from that used in Ref. [8], where the inferred quadrature variances are equivalent to measurements of $\Delta^2_{\text{inf}}\hat{X}_2 = \Delta^2(\hat{X}_1 - \hat{X}_2)$ and $\Delta^2_{\text{inf}}\hat{Y}_2 = \Delta^2(\hat{Y}_1 + \hat{Y}_2)$ [11]. This choice is different in that it does not give the optimal violation of Eq. (6) [6]; however, in the parameter regime we consider the difference between the choices of inferred quadratures is not qualitatively significant.
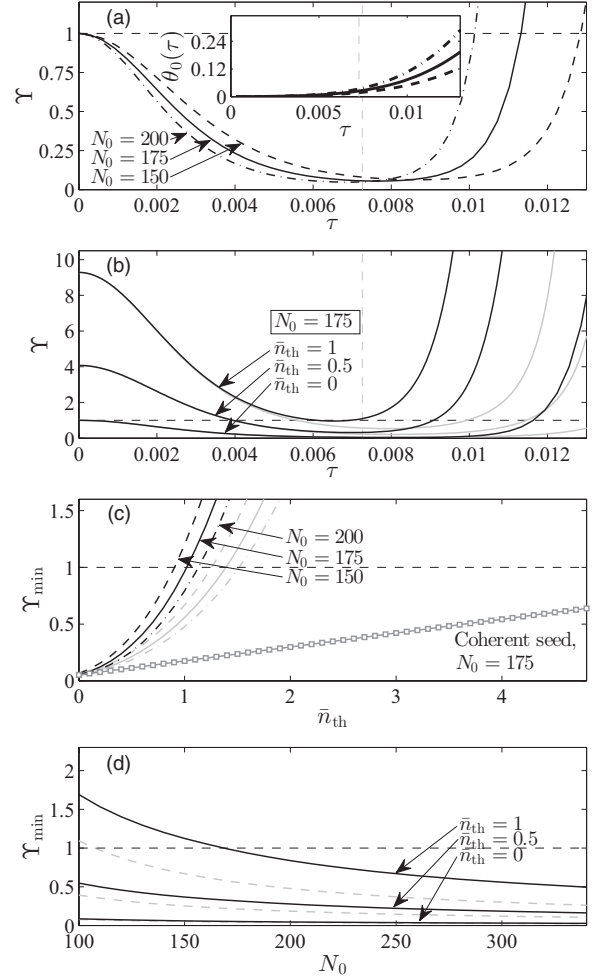

FIG. 2. (a) Evolution of the EPR entanglement parameter Υ for the same situation as in Fig. 1(a). The EPR criterion corresponds to $\Upsilon < 1$ (dashed horizontal line). The inset shows the evolution of the optimal phase angle of the local oscillator $\theta_0(\tau)$ for each N_0. (b) Evolution of Υ for thermally seeded signal and idler modes and $N_0 = 175$. The experimental measurement time $\tau' = 0.0073$ is shown in (a) and (b) as a vertical dotted line. The respective gray lines are the analytic predictions from the undepleted pump model. (c) Time-optimized EPR parameter Υ_{min} as a function of $\bar{n}_{\text{th}}$ for different N_0. The respective gray lines are the analytic predictions from the undepleted pump model. The gray line with squares shows Υ_{min} for $N_0 = 175$, but assuming that the seeds are in a coherent state (sharing initially the same phase as the pump mode) with average populations of $|\alpha_{\pm 1}(0)|^2 = \bar{n}_{\text{th}}$. (d) Same as in (c), but as a function of N_0 for three different thermal seeds $\bar{n}_{\text{th}}$.

the method used in Ref. [8], where an atomic three-port beam splitter is used to measure relevant quadratures.

Phase accrued due to $\hat{H}_{\text{el}} + \hat{H}_Z$ leads to a drifting in the phase relation between the local oscillator and the signal and idler modes. This means that our original quadrature choice of $\hat{X}_j(\pi/4)$ and $\hat{X}_j(3\pi/2)$ may not measure the optimal violation of the EPR criterion. By minimizing this criterion as a function of phase the optimal choice of quadratures becomes $\hat{X}_j(\theta_0(\tau))$ and $\hat{X}_j(\theta_0(\tau) + \pi/2)$, where $\theta_0(\tau)$ is the optimal local oscillator phase relative to the signal and idler modes.
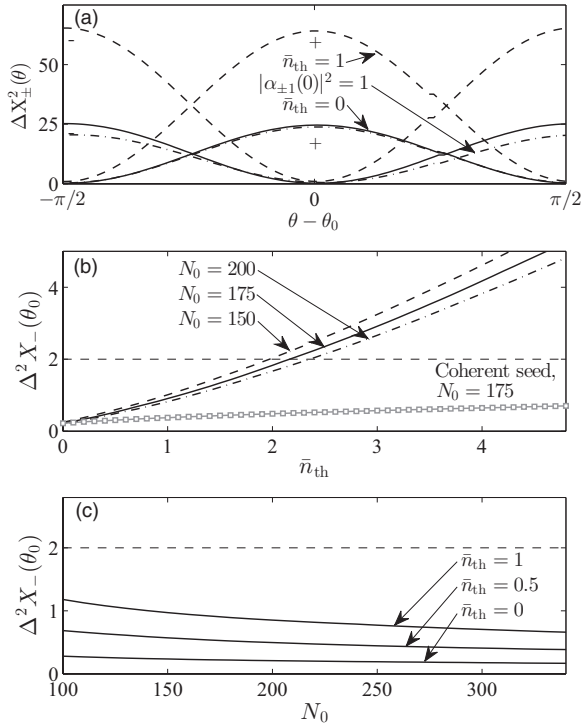
FIG. 3. (a) Two-mode quadrature variances $\Delta^2 \hat{X}_\pm(\theta)$ at $\tau' = 0.0073$ as functions of the local oscillator phase angle $\theta - \theta_0$ for vacuum (solid lines) and thermally seeded (dashed lines) signal and idler modes; $N_0 = 175$ in both cases. We also include a calculation of $\Delta^2 \hat{X}_-(\theta)$ for a comparable coherent seed (dot-dashed line) $|\alpha_{\pm 1}(0)|^2 = 1$, which is almost indistinguishable from the vacuum case. (b) Time-optimized minimum of $\Delta^2 \hat{X}_-(\theta_0)$ as a function of $\bar{n}_{th}$ for different N_0. The gray line with squares shows $\Delta^2 \hat{X}_-(\theta_0)$ for $N_0 = 175$, but assuming the seeds are in a coherent state with average populations of $|\alpha_{\pm 1}(0)|^2 = \bar{n}_{th}$. (c) Same as in (b), but as a function of N_0 for different $\bar{n}_{th}$.

In Fig. 2(a) we show the results of calculation of the phase-optimized EPR-entanglement parameter Υ (with $\Upsilon_{-1} = \Upsilon_1 \equiv \Upsilon$ due to the symmetry of the signal and idler modes) for the signal and idler modes initially in a vacuum state. We see that strong EPR entanglement ($\Upsilon < 1$) can be achieved for a large experimental time frame, up to $\tau \simeq 0.01$; more specifically, we predict suppression of the optimal EPR entanglement of at least 90% below unity for all relevant total atom numbers (ranging from 150 to 200) at $\tau' = 0.0073$. Unlike the simple undepleted pump model, which predicts $\Upsilon = \cosh^{-2}(2N_0\tau)$ and hence indefinite suppression of the EPR criterion [21], EPR entanglement in the full model is eventually lost due to a combination of back-conversion ($|+1\rangle + |-1\rangle \rightarrow |0\rangle + |0\rangle$) and the loss of coherence in the pump mode.

Our results predict that a strong EPR violation should have been observed if the signal and idler modes were indeed generated from an initial vacuum state. In light of this and the large error margin of the experimental result in Ref. [8], which thus cannot conclusively demonstrate the existence or nonexistence of EPR entanglement, we now discuss the possible presence of stray or thermally excited atoms in the signal and idler modes and the effects such seeding can have on entanglement and particularly the EPR criterion. The
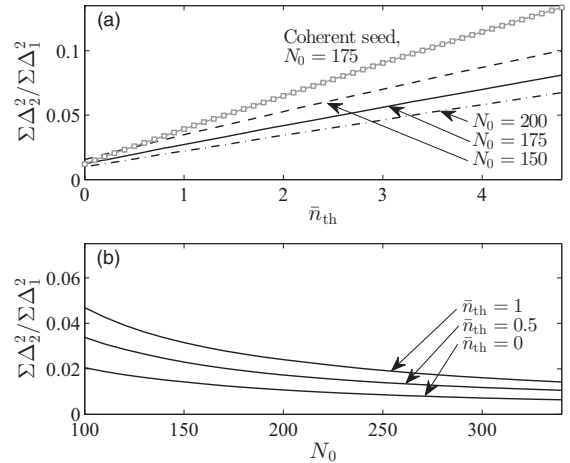

FIG. 4. (a) Time-optimized inseparability criterion for the quadrature entangled state, quantified via $\sum \Delta_2^2 / \sum \Delta_1^2 < 1$, as a function of $\bar{n}_{th}$ for different N_0. The gray line with squares shows $\sum \Delta_2^2 / \sum \Delta_1^2$ for $N_0 = 175$, but assuming the seeds are in a coherent state with average populations $|\alpha_{\pm 1}(0)|^2 = \bar{n}_{th}$. (b) Same as in (a), but as a function of N_0 for different $\bar{n}_{th}$.

results of calculation of the EPR-entanglement parameter Υ for an initial thermal seed of $\bar{n}_{th}$ in both modes are shown in Figs. 2(b)–2(d). We find that the introduction of a thermal seed reduces the strong correlation between the signal and idler modes, leading to an eventual loss of EPR entanglement. For an initial number of atoms in the pump mode ranging between 150 and 200, EPR entanglement is lost already for $\bar{n}_{th} \simeq 1$. Direct experimental detection of stray atoms at such a low population level is beyond the current resolution of absorption imaging techniques [8]. More generally, our numerical results show that the maximum $\bar{n}_{th}$ that can be tolerated while preserving the EPR entanglement scales as $(\bar{n}_{th})_{max} \sim 0.06 N_0^{11/20}$ in the range of $100 \lesssim N_0 \lesssim 400$ (see the Appendix for further discussion). For comparison, seeding the signal and idler modes with a coherent state [13] of similar population does not have such a dramatic effect on EPR entanglement [see the gray line with squares in Fig. 2(c)].

C. Quadrature squeezing and inseparability

To further highlight the high sensitivity of EPR entanglement to initial thermal noise we contrast it with two other weaker measures of the nonclassicality of the state: two-mode quadrature squeezing and intermode entanglement in the sense of inseparability, which were the main focus of Ref. [8]. The two-mode quadrature variances are defined as $\hat{X}_\pm(\theta) = \hat{X}_1(\theta) \pm \hat{X}_{-1}(\theta)$, with $\Delta^2 \hat{X}_-(\theta) < 2$ corresponding to two-mode squeezing [21], i.e., suppression of fluctuations below the level dictated by a minimum-uncertainty state. We plot the results of our numerical calculations of quadrature variances in Fig. 3(a). From these results we observe that the measurements of Ref. [8] do not agree with the amplitude of the oscillation that we find for an initial vacuum state (solid lines) or a small coherent seed (dot-dashed line). Rather they suggest the presence of a small thermal seed of $\bar{n}_{th} \simeq 1$ (dashed lines), although for definitive differentiation of initial thermal or coherent populations further experimental measurements

with reduced error margins are required. Further, calculation of the minimum of $\Delta^2 \hat{X}_-$ [Figs. 3(b) and 3(c)] highlights that two-mode squeezing is preserved for thermal seed populations up to $\bar{n}_{th} \simeq 1.7$, which is consistent with our interpretation of the measurements reported in Ref. [8].

Next we define the sum of single-mode quadrature variances as $\sum \Delta_1^2 = 2(\Delta^2 \hat{X}_1 + \Delta^2 \hat{Y}_1)$ and the sum of two-mode quadrature variances $\sum \Delta_2^2 = \Delta^2 \hat{X}_- + \Delta^2 \hat{Y}_+$. [Following the treatment of Ref. [8], we calculate the single-mode quadrature variances with the standard definition of quadratures $\hat{X}_j(\theta) = \hat{a}_j e^{-i\theta} + \hat{a}_j^\dagger e^{i\theta}$.] Inseparability of the produced $m_F = \pm 1$ pair-entangled state is equivalent to $\sum \Delta_2^2 / \sum \Delta_1^2 < 1$ [24]. Figures 4(a) and 4(b) demonstrate that this measure of entanglement is far less sensitive to the presence of a thermal seed in comparison to the stronger criterion of EPR entanglement. Also, unlike the EPR criterion, this inseparability measure does not significantly differentiate between coherent and thermal seeding.

IV. SUMMARY

In conclusion, we have demonstrated that for an initial vacuum state in the signal and idler modes a strong suppression of the EPR criterion can be achieved in the parameter regime of Ref. [8], most importantly including the experimental measurement time of $\tau' = 0.0073$. However, we also establish that the strength of EPR entanglement depends crucially on the nature of the initial spin fluctuations. Specifically, we predict that for a pump mode of initially 150–200 atoms, a thermal initial seed of $\bar{n}_{th} \simeq 1$ is sufficient to rule out EPR entanglement. Weaker measures of entanglement, such as inseparability, are still possible to observe as these are far more robust to thermal noise. This implies that spin-changing collisions may still be a good source of entanglement even in the presence of large thermal effects, even though we may not be able to carry through the EPR arguments that confront the completeness of quantum mechanics and advocate for local hidden-variable theories. Importantly, our results suggest that the measurement of this EPR criterion can serve as a sensitive probe of the initial state, which triggers the pair-production process, beyond measures employed in Ref. [13]. This understanding of the sensitivity of EPR entanglement to initial thermal noise will hopefully lead to refining of spin-mixing experiments towards demonstration

of the EPR paradox with massive particles. We expect our findings to be also relevant to related proposals based on molecular dissociation [25], condensate collisions [26–29], and optomechanical systems [30].

APPENDIX: UNDEPLETED PUMP APPROXIMATION

To invoke the undepleted pump approximation, we assume that the pump mode is initially in a coherent state with an amplitude $\alpha_0(0) = \sqrt{N_0}$ (which we choose to be real without loss of generality) and that it does not change with time. By additionally choosing the quadratic Zeeman effect to be phase matched ($q = gN_0$), we can reduce the model Hamiltonian to that of optical parametric down-conversion [21] $\hat{H} = \hbar \chi (\hat{a}_1^\dagger \hat{a}_{-1}^\dagger + \text{H.c.})$, in which $\chi = gN_0$. The Heisenberg equations of motion following from this are $d\hat{a}_{\pm 1}/d\tau = -iN_0 \hat{a}_{\mp 1}^\dagger$, where $\tau = gt$ is a dimensionless time. Solutions to these equations are given by

$$\hat{a}_{\pm 1}(\tau) = \cosh(N_0\tau)\hat{a}_{\pm 1}(0) - i \sinh(N_0\tau)\hat{a}_{\mp 1}^\dagger(0), \quad \text{(A1)}$$

which are physically valid in the short-time limit, generally corresponding to less than 10% depletion of the pump mode occupation.

Considering specific initial states for the signal and idler modes, these solutions can be used to calculate expectation values of various quantum mechanical operators and observables. For example, for a thermal initial state with an equal population in both modes, $\langle \hat{a}_1^\dagger(0)\hat{a}_1(0)\rangle = \langle \hat{a}_{-1}^\dagger(0)\hat{a}_{-1}(0)\rangle \equiv \bar{n}_{th}$, the subsequent evolution of the mode populations is given by

$$\langle \hat{a}_{\pm 1}^\dagger(\tau)\hat{a}_{\pm 1}(\tau)\rangle = \sinh^2(N_0\tau)[1 + 2\bar{n}_{th}] + \bar{n}_{th}, \quad \text{(A2)}$$

whereas the anomalous moments evolve according to

$$\langle \hat{a}_{\pm 1}(\tau)\hat{a}_{\mp}(\tau)\rangle = -i \sinh(N_0\tau)\cosh(N_0\tau)[1 + 2\bar{n}_{th}]. \quad \text{(A3)}$$

Similarly, the EPR-entanglement parameter is found to be given by

$$\Upsilon \cong \left[\frac{(1 + 2\bar{n}_{th})^2 + \frac{1}{N_0}[(1 + 2\bar{n}_{th})\cosh(2N_0\tau) - 1][2(1 + 2\bar{n}_{th})\cosh(2N_0\tau) - 1]}{(1 + 2\bar{n}_{th})\cosh(2N_0\tau) - \frac{1}{N_0}[(1 + 2\bar{n}_{th})\cosh(2N_0\tau) - 1]^2} \right]^2, \quad \text{(A4)}$$

where we have assumed $N_0 \gg 1$. The minimum value of this quantity (with respect to time τ) gives the maximal violation of the EPR criterion

$$\Upsilon_{min} \cong \left[\frac{\sqrt{2N_0}}{\sqrt{\frac{1}{2}N_0 - (1 + 2\bar{n}_{th}) - \frac{1}{2N_0}\{(1 + 2\bar{n}_{th})^3 - [(1 + 2\bar{n}_{th})^2 + 1]\sqrt{2N_0}\}}} - 2 \right]^2, \quad \text{(A5)}$$

which is achieved at the optimal time

$$\tau_{min} = \frac{1}{2N_0} \text{arccosh}\left[-\frac{1}{2}(1 + 2\bar{n}_{th}) + \frac{1}{2}\sqrt{(1+2\bar{n}_{th})^2 + 2N_0} \right]. \quad \text{(A6)}$$

From Eq. (A5) we also determine the maximum allowable thermal population before EPR entanglement is lost. By numerical analysis we find a maximum seed of $(\bar{n}_{\text{th}})_{\text{max}} \simeq 0.05 N_0^{2/3}$ in the range $100 \leqslant N_0 \leqslant 400$. We find that this compares reasonably with the results of full numerical simulations, which predict $(\bar{n}_{\text{th}})_{\text{max}} \simeq 0.06 N_0^{11/20}$. Furthermore, we may also calculate the minimum two-mode quadrature variance

$$\Delta^2 X_- = 2(1 + 2\bar{n}_{\text{th}})[\cosh(2N_0\tau) - \sinh(2N_0\tau)] \qquad \text{(A7)}$$

and the intermode inseparability parameter (see the main text)

$$\Sigma \Delta_2^2 / \Sigma \Delta_1^2 = 1 - \tanh(2N_0\tau). \qquad \text{(A8)}$$

Despite their limited applicability and the quantitative disagreement with the numerical results, the analytic predictions of the undepleted pump approximation give useful insights into the qualitative aspects of different measures of entanglement. For example, to leading order, Eqs. (A4) and (A7) predict, respectively, quadratic and linear growth of the EPR entanglement parameter and two-mode squeezing with the thermal seed $\bar{n}_{\text{th}}$, whereas the intermode inseparability (A8) is insensitive to $\bar{n}_{\text{th}}$. The predictions for EPR entanglement and two-mode squeezing are in qualitative agreement with the numerical results discussed in the main text, while we find that weak linear growth with $\bar{n}_{\text{th}}$ emerges for intermode inseparability due to depletion of the pump. These qualitative predictions highlight the lower tolerance and higher sensitivity of the EPR entanglement to thermal noise.

[1] E. Schrödinger, Math. Proc. Cambridge Philos. Soc. **31**, 555 (1935).

[2] V. Giovannetti, S. Lloyd, and L. Maccone, Science **306**, 1330 (2004).

[3] C. Gross, T. Zibold, E. Nicklas, J. Estève, and M. K. Oberthaler, Nature (London) **464**, 1165 (2010); M. F. Riedel, P. Böhi, Y. Li, T. W. Hänsch, A. Sinatra, and P. Treutlein, *ibid.* **464**, 1170 (2010).

[4] A. Einstein, B. Podolsky, and N. Rosen, Phys. Rev. **47**, 777 (1935); N. Bohr, *ibid.* **48**, 696 (1935).

[5] D. Bohm, Phys. Rev. **85**, 166 (1952); D. Bohm and Y. Aharonov, *ibid.* **108**, 1070 (1957); J. S. Bell, Physics **1**, 195 (1964).

[6] M. D. Reid, Phys. Rev. A **40**, 913 (1989).

[7] Z. Y. Ou, S. F. Pereira, H. J. Kimble, and K. C. Peng, Phys. Rev. Lett. **68**, 3663 (1992).

[8] C. Gross, H. Strobel, E. Nicklas, T. Zibold, N. Bar-Gill, G. Kurizki, and M. K. Oberthaler, Nature (London) **480**, 219 (2011).

[9] H. Pu and P. Meystre, Phys. Rev. Lett. **85**, 3987 (2000).

[10] L.-M. Duan, A. Sørensen, J. I. Cirac, and P. Zoller, Phys. Rev. Lett. **85**, 3991 (2000).

[11] A. J. Ferris, M. K. Olsen, E. G. Cavalcanti, and M. J. Davis, Phys. Rev. A **78**, 060104 (2008).

[12] M. Melé-Messeguer, B. Juliá-Díaz, A. Polls, and L. Santos, Phys. Rev. A **87**, 033632 (2013).

[13] C. Klempt, O. Topic, G. Gebreyesus, M. Scherer, T. Henninger, P. Hyllus, W. Ertmer, L. Santos, and J. J. Arlt, Phys. Rev. Lett. **104**, 195303 (2010).

[14] C. K. Law, H. Pu, and N. P. Bigelow, Phys. Rev. Lett. **81**, 5257 (1998).

[15] H. Pu, C. K. Law, S. Raghavan, J. H. Eberly, and N. P. Bigelow, Phys. Rev. A **60**, 1463 (1999).

[16] M.-S. Chang, Q. Qin, W. Zhang, L. You, and M. S. Chapman, Nat. Phys. **1**, 111 (2005).

[17] Y. Kawaguchi and M. Ueda, Phys. Rep. **520**, 253 (2012).

[18] J. Kronjäger, C. Becker, M. Brinkmann, R. Walser, P. Navez, K. Bongs, and K. Sengstock, Phys. Rev. A **72**, 063619 (2005).

[19] S. Bize, Y. Sortais, M. S. Santos, C. Mandache, A. Clairon, and C. Salomon, Europhys. Lett. **45**, 219 (1999).

[20] J. Kronjäger, C. Becker, P. Navez, K. Bongs, and K. Sengstock, Phys. Rev. Lett. **97**, 110404 (2006).

[21] D. Walls and G. Milburn, *Quantum Optics* (Springer, Berlin, 2008).

[22] This method can be easily implemented for modeling the pump mode being initially in either a pure Fock state or a coherent state. For the large values of N_0 and relatively small time durations considered in this paper, the two alternatives give very similar results; accordingly, we restrict ourselves to presenting the results only for the coherent initial state.

[23] M. Olsen and A. Bradley, Opt. Commun. **282**, 3924 (2009).

[24] M. G. Raymer, A. C. Funk, B. C. Sanders, and H. de Guise, Phys. Rev. A **67**, 052104 (2003).

[25] K. V. Kheruntsyan, M. K. Olsen, and P. D. Drummond, Phys. Rev. Lett. **95**, 150405 (2005); K. V. Kheruntsyan, Phys. Rev. A **71**, 053609 (2005).

[26] A. J. Ferris, M. K. Olsen, and M. J. Davis, Phys. Rev. A **79**, 043634 (2009).

[27] J.-C. Jaskula, M. Bonneau, G. B. Partridge, V. Krachmalnicoff, P. Deuar, K. V. Kheruntsyan, A. Aspect, D. Boiron, and C. I. Westbrook, Phys. Rev. Lett. **105**, 190402 (2010).

[28] K. V. Kheruntsyan, J.-C. Jaskula, P. Deuar, M. Bonneau, G. B. Partridge, J. Ruaudel, R. Lopes, D. Boiron, and C. I. Westbrook, Phys. Rev. Lett. **108**, 260401 (2012).

[29] J. Kofler, M. Singh, M. Ebner, M. Keller, M. Kotyrba, and A. Zeilinger, Phys. Rev. A **86**, 032115 (2012).

[30] D. Vitali, S. Gigan, A. Ferreira, H. R. Böhm, P. Tombesi, A. Guerreiro, V. Vedral, A. Zeilinger, and M. Aspelmeyer, Phys. Rev. Lett. **98**, 030405 (2007); H. Müller-Ebhardt, H. Miao, S. Danilishin, and Y. Chen, arXiv:1211.4315.